Bulletin of Earthquake Engineering (2019) 17:439–471
https://doi.org/10.1007/s10518-018-0455-0

ORIGINAL RESEARCH

Numerical simulation of potential seismic pounding among adjacent buildings in series

Shehata E. Abdel Raheem[1,2] · **Mohammed Y. M. Fooly**[2] · **Aly G. A. Abdel Shafy**[2] · **Ahmed M. Taha**[1] · **Yousef A. Abbas**[2] · **Mohamed M. S. Abdel Latif**[2]

Received: 25 September 2017 / Accepted: 17 August 2018 / Published online: 20 August 2018

Abstract

Numerous urban seismic vulnerability studies have recognized pounding between adjacent structures as one of the main risks for neighbouring buildings due to the restricted separation distance. The seismic pounding could produce damages that range from slight non-structural to serious structural damage that could even head to a total collapse of buildings. Therefore, an assessment of the seismic pounding risk of buildings is indispensable in future calibration of seismic design code provisions. Thus, this study targets to draw useful recommendations for seismic design through the evaluation of the pounding effects on adjacent buildings. A numerical simulation is formulated to estimate the pounding effects on the seismic response demands of three adjacent buildings in series with different alignment configurations. Three adjacent buildings of 3-storey, 6-storey and 12-storey MRF buildings are combined together to produce three different alignment configurations; these configurations of adjacent buildings are subjected to nine ground motions that are absolutely compatible with the design spectrum. The nonlinear time-history is performed for the evaluation of the response demands of different alignment configurations of the adjacent buildings using structural analysis software ETABS. Various response parameters are investigated such as displacement, acceleration, storey shear force mean and maximum responses, impact force and hysteretic behaviour. Based on the obtained results, it has been concluded that the severity of the seismic pounding effects depends on the vibration characteristic of the adjacent buildings, the input excitation characteristic and whether the building has interior or exterior alignment position, thus either exposed to one or two-sided impacts. Seismic pounding among adjacent buildings induces greater shear force and acceleration response demands at different story levels for the high rise building, while the response could be reduced in the short buildings compared to that of no-pounding case. The effect of poundings of adjacent buildings seems to be critical for most of the cases and, therefore, the structural pounding phenomenon is rather detrimental than beneficial.

Keywords Adjacent buildings in series · Seismic pounding · Time history analysis · Separation gap · Response demands · Earthquake characteristics

✉ Shehata E. Abdel Raheem
shehataraheem@yahoo.com

Extended author information available on the last page of the article

1 Introduction

The buildings in many highly congested municipal cities constitute a foremost concern for seismic pounding damage. Urban seismic vulnerability inspections after several major earthquakes have recognized pounding as one of the main hazards to buildings and bridges (Rosenblueth 1986; Bertero 1987; Kasai and Maison 1991; Jeng and Tzeng 2000; Abdel Raheem 2006, 2009; Kawashima et al. 2011; Cole et al. 2010, 2012; Abdel Raheem and Hayashikawa 2013; Inel et al. 2013). The majority of building codes suggest separation distances based on maximum lateral displacements of each building or height of buildings in order to provide safety gap size between them. Although numerous recent codes require a minimum seismic separation gap, it is as yet insufficient as codes essentially lag behind the recent research (ICBO 1997; IS 2002; ECS 2004; ICC 2009; ASCE 2010). Pounding damage was inspected during the 1940 Elcentro earthquake, the 1985 Mexico earthquake, the 1988 Seguenay earthquake, the 1992 Cairo earthquake, the 1994 Northridge earthquake, the 1995 Kobe earthquake, the 1999 Kocaeli earthquake and the 2011 Van earthquake. In the Mexico City catastrophic earthquake, around 40% of the damaged structures faced certain level of pounding and structural collapse for 15% of them are observed (Rosenblueth 1986; Anagnostopoulos and Karamaneas 2008). In the 1989 Loma Prieta earthquake, more than 200 pounding incidents through over 500 buildings were revealed at sites over 90 km from the epicentre (Kasai and Maison 1997), thus endorsing the potential disastrous damages in the future earthquakes. Pounding among adjacent buildings in series could have more destruction as nearby buildings have out of phase vibration characteristics and insufficient separation gap or lack of mitigation measure of energy dissipation system to accommodate the relative deformation of adjacent buildings. Examination of structural pounding damage during recent earthquakes (Cole et al. 2012; Naserkhaki et al. 2013; Efraimiadou et al. 2013; Abdel Raheem 2013a, b, 2014) has identified building configuration categories that are susceptible to pounding damage: equal story height pounding; non-equal story height pounding; heavier adjacent buildings pounding; eccentric pounding and buildings in series, insufficient seismic separation gap between buildings allows them to pound and damage each other. The collision between adjacent structures may lead to a significant increase of the response of the lighter structure as well as may result in a substantial increase of the range and intensity of damage at the base of the structure, whereas the behaviour of the heavier main building has been found to be only slightly influenced by structural interactions (Jankowski 2009). Favvata (2017) investigated the seismic pounding between the adjacent buildings with un-equal story heights to determine the minimum required separation gap for adjacent RC frames with potential inter-story seismic pounding for complete avoidance of the contact between the adjacent structures. From the literature review, contradictory conclusions are found. Papadrakakis and Mouzakis (1995) concluded, on the basis of a shake table test and numerical simulations, that pounding resulted in displacement amplification and reduction of the stiffer and more flexible buildings, respectively. Nonetheless, Jankowski (2010) observed, with another experiment, that this conclusion could be challenged if the mass of the more flexible structure is much bigger than that of the more rigid structure.

The seismic pounding of adjacent buildings has been thoroughly investigated by using several structural and impact models (Davis 1992; Jankowski 2006; Mahmoud and Jankowski 2011; Abdel Raheem 2014; Abdel Raheem et al. 2018b). The pounding among adjacent structures in series during earthquakes causes a repeated hammer that is exerted on each other, hence could lead to damages that ranges from slight non-structural local damage to serious structural global damage that could prompt buildings total failure, Fig. 1. The damage due to end building pounding of adjacent buildings in series is a standout amongst the most widely recognized vulnerabilities as urban areas are brimming with line alignment of slightly separated or in contact buildings (Jeng and Tzeng 2000; Bull et al. 2010). Anagnostopoulos (1988) investigated the pounding among adjacent buildings in series using idealized single degree of freedom systems and linear viscoelastic impact model, it was concluded that the exterior buildings are much more severely penalized than the interior buildings, the response of interior building was observed to be increased or decreased relying upon whether it has a smaller or higher fundamental period than the adjacent structures; stiffer structures usually display an amplified response, while the flexible structures encountering a response reduction. The stiffer structure within the line alignment got less magnification than their external location. Athanassiadou et al. (1994) did comparable reproductions on the ground motion phase shift effect; it is observed that the stiffer structure, irrespective of its relative alignment position, undergone the most response magnification. Anagnostopoulos and Spiliopoulos (1992) concluded based on numerical simulation of three buildings that occasionally pounding generated higher response amplification for external building position than for internal building. In contrast, damage assessment analysis in Christchurch 2011 earthquake displayed various situations where the interior structures of a straight alignment were seriously damaged, while the exterior structures of the same alignment endured (Cole et al. 2011). A shake table examination on pounding interaction among buildings in series (Khatiwada and Chouw 2013) has recognized that an external building alignment is extremely vulnerable to pounding damage, while interior buildings could be safer. Despite the extensive research carried out on the seismic collision of buildings during the last two decades, which has been mainly reported earlier, the findings of many works have been refuted by other pertinent studies. This discrepancy has to do with the high level of complexity inherent in the problem (Cole et al. 2010; Efraimiadou et al. 2013). Therefore, it is required to evaluate the seismic pounding effect on buildings response demands to promote an improved damage control and more competent utilization of land. Hence, the purpose of this detailed pounding analysis was to provide the basic information to set up guidelines for potential pounding damage evaluation.

This study focuses on the seismic pounding effects on the seismic response demands among adjacent buildings in series with equal story heights, where the pounding predominantly affects the global and local responses demands. A nonlinear finite element

The 1985 Mexico Earthquake (Anagnostopoulos 1988) | The 1985 Mexico earthquake (Johnmartin 2018, NCEI 2018) | The 2011 Van earthquake (Ozmen et al. 2013, Aykutozdemir 2018)

Fig. 1 Pounding damage in adjacent buildings of different heights modelling is developed for the formulation of the pounding among adjacent buildings in series. Three 3-storey, 6-storey and 12-storey MRF buildings are combined together to produce three different alignment configurations of three adjacent buildings in series. These configurations of buildings are subjected to nine ground motions that are absolutely compatible with the design spectrum. The nonlinear time history analysis is used to evaluate potential pounding among adjacent buildings in series under earthquake hazard. The effect of collision is studied for different separation distances; three alignment configurations under nine ground motions, and then compared with no-pounding model. The nonlinear time-history responses of these MRF buildings are evaluated by means of the structural analysis software ETABS. Various responses demands are investigated such as maximum displacements, acceleration, impact force and storey shear force. The mean and maximum values from all the seismic demands for nine earthquake excitations are presented, where the extreme effect of the structural pounding on the seismic performances of the structures is identified. The severity of the impact depends on the dynamic characteristics of the adjacent buildings, the input excitation characteristics, and the position of building alignment whether it is subjected to one or two-sided impacts.

2 Numerical modelling for seismic simulation

2.1 Nonlinear dynamic analysis procedures

The nonlinear time-history responses of the MRF buildings are evaluated by means of the structural analysis software ETABS (CSI 2013, 2016), where the geometric and material nonlinearities are considered during structural FE modelling and analysis. The equilibrium equations for nonlinear static and nonlinear time history analysis take into account the deformed configuration of the structure. The material nonlinearity could be captured with the inelastic behaviour in the form of a nonlinear force–deformation relation, which affords insight into ductility and limit-state behaviour. The concrete and steel constitutive models used in the analysis are shown in Fig. 2. Beam-column elements with plastic hinges at both ends (flexural hinges in beams, biaxial axial-flexural hinges in columns) have been used for the structural members of the nonlinear models, where the length of the plastic hinges is assumed equal to the height of the section. In the FE model, a bi-linear model issued for the modelling of steel reinforcement, which can consider the strain-hardening effect. Mander stress–strain curve is assigned to concrete material section for confined and unconfined compression and tension stress–strain relation (Mander et al. 1988). The yielding

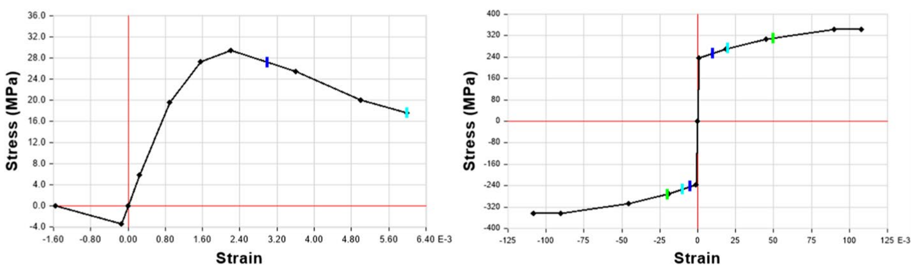

Fig. 2 Concrete stress–strain and steel constitutive models used in the analysis

and post-yielding behaviour can be modelled using plastic hinges. Hinge properties can be computed automatically from the element material and section properties according to FEMA-356 (FEMA 2000) or ASCE 41-13 criteria (ASCE 2013). The fiber P-M2-M3 hinge models the axial behaviour of a number of representative axial fibers distributed across the cross section of the frame element.

2.2 Input earthquake excitation

For the nonlinear dynamic analysis of the seismic pounding among adjacent buildings in series, a set of nine-ground motion time histories is chosen for grasping the input excitation effect. The input excitation in the form of acceleration time histories is required to be well-matched with the design response spectra at the target site. A time domain scaling method is used to scale the selected real ground motion records (PEER 2013) to match the proposed elastic design spectrum (ECP 2008) using SeismoMatch software (Abrahamson 2006). The real and matched ground motion spectra are plotted against design response spectrum as shown in Fig. 3. For the response-history analysis, the key parameters as indicator of the damage potential of the earthquake excitation are calculated for real and matched ground motion records and presented in Table 1. The ground motions scaling based on time domain wavelet spectral matching approach is achieved through an adjustment of the time history in the time domain by adding wavelets to the acceleration time-series. Wavelet adjustment of recorded accelerograms has the same advantages as the Fourier adjustment methods but leads to a more focused correction in the time domain thus introducing less energy into the ground motion and also preserves the non-stationary characteristics of the original ground motion. This method preserves the overall phasing characteristics and as the time varying frequency content of the ground motion (Somerville 1998). Scaling the ground motions is carried out in accordance with the provisions of seismic codes (Shome et al. 1998; BSSC 2009; ASCE 2010). In this study, The ground motions are scaled such that the average value of the 5% damped response spectra for the suite of motions is not less than the design response spectrum for the site for periods ranging from $0.2T_1$ to $1.5T_2$ (0.08–3.0 s), where T_1 and T_2 are the shortest and longest fundamental period of the adjacent buildings in the fundamental vibration mode for the direction of response being analyzed. According to ASCE7-10 Section 17.6.3.4: The average value of the measured response parameter of interest is permitted to be used for design, if seven or more pairs of ground motions are used for the response-history analysis, if fewer than seven

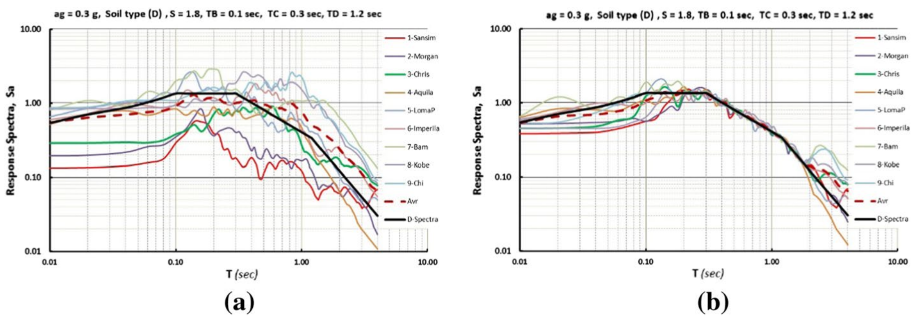

Fig. 3 Response spectra of the various earthquakes considered along with the design response spectrum (ECP 2008). **a** Real ground motion records, **b** matched ground motion records

Table 1 Key parameters of real and matched nine-ground motion records

Earthquake/station	Mw	Spectra match	PGA (g)	PGV (m/s)	PGD (cm)	Specific energy density (cm^2/s)	Arias intensity	Housner intensity	Period Ts (s)
San Simeon, CA./RSN3994-36153090	6.52	Real	0.13	13.10	7.72	497.3	0.21	40.29	0.13
		Match	0.38	33.80	7.93	1133.6	1.27	123.0	0.38
Morgan Hill, USA/RSN457-G03000	6.19	Real	0.19	11.02	3.12	500.3	0.34	48.6	0.19
		Match	0.52	26.20	4.32	856.3	1.42	118.8	0.48
Christchurch, NZ/RSN8124-RHSCN86 W	6.20	Real	0.29	33.52	16.99	1479.6	1.13	100.56	0.29
		Match	0.45	37.20	18.14	1667.6	1.82	140.41	0.45
L'Aquila, Italy/RSN4481-FA030YLN	6.30	Real	0.52	35.91	4.47	565.9	1.37	91.60	0.51
		Match	0.63	43.62	3.68	714.3	2.08	111.69	0.62
Loma Prieta, USA/RSN811-WAH090	6.93	Real	0.65	38.12	5.91	1487.2	6.27	128.35	0.64
		Match	0.60	35.35	5.69	1299.5	5.90	119.80	0.58
Imperial Valley, USA/RSN160-H-BCR140	6.53	Real	0.60	46.75	20.22	2655.4	3.97	174.64	0.59
		Match	0.57	40.62	15.79	1721.5	2.92	126.76	0.56
Bam, Iran/RSN4040-BAM-L	6.60	Real	0.81	124.12	33.94	7989.2	7.83	389.31	0.79
		Match	0.65	64.89	20.07	2802.4	4.80	147.44	0.64
Kobe, Japan/RSN1106-KJM000	6.90	Real	0.83	91.11	21.11	7581.8	8.38	363.11	0.82
		Match	0.45	36.94	12.33	2054.2	2.29	139.71	0.44
Chi-Chi, Taiwan/RSN1231-CHY080-N	7.62	Real	0.86	93.16	41.66	10,247.2	6.41	395.38	0.85
		Match	0.53	37.16	39.54	3786.0	1.88	141.20	0.52

pairs of ground motions are used, the maximum value of the response parameter of interest shall be used for design.

2.3 Building physical model

The building construction industry in Egypt had broadly used medium-rise RC buildings having twelve stories, the height limit authorized by the local authorities in most regions. These buildings are constructed with diverse patterns and structural systems. Three models for typical buildings with three, six and twelve stories are selected as shown in Fig. 4. The buildings have story height 3 m for all floors and bay width 5 m in both directions. Concrete with compressive strength $f_c = 30$ MPa, unit weight $\gamma_c = 25$ kN/m^3, modulus of elasticity $E_c = 24$ GPa, Poisson's ratio $\upsilon = 0.2$ and reinforcing steel with yield strength $F_y = 360$ MPa are used for analysis and design. The design process requires the determination of the loads that act on the RC buildings. The gravity loads include dead loads (DL) and live loads (LL); and lateral loads include earthquake loads. The dead loads take account of the own weight of the structural components, the weight of flooring cover (1.5 kN/m^2) and panel wall loads intensity of 10 kN/m on all beams. A live load of 2 kN/m^2 is selected for the residential buildings. The seismic design of the studied buildings has been done according to ECP-201 (ECP 2007, 2008), with design parameters: importance factor $\gamma = 1$; earthquake zone (5B) based on Egyptian zoning system; peak ground acceleration PGA = 0.3 g; Type 1 design response spectrum; soil class (D) and soil factor S = 1.8. The reduction factor, R = 5, is selected for MRF buildings. All structural elements of the buildings are designed, where the floor has slab–beam system with 0.15 m slab thickness and 0.3 × 0.7 m dropped beam. The dimensions and reinforcement of column elements for the studied buildings are presented in Table 2. The capacity design rules are adopted, where the brittle failure or other harmful failure mechanisms (plastic hinges in columns, shear failure of structural elements, failure of beam-column joints, yielding of foundations) shall be prohibited, through definition of the design actions through selected regions from equilibrium conditions, such that plastic hinges with their possible over-strengths have been created in their adjacent areas (ECP 2007; ECS 2004). For the MRF structural systems, the capacity design condition should be fulfilled at all beam-column joints:

$$\sum M_{RC} \geq 1.3 \sum M_{Rb} \tag{1}$$

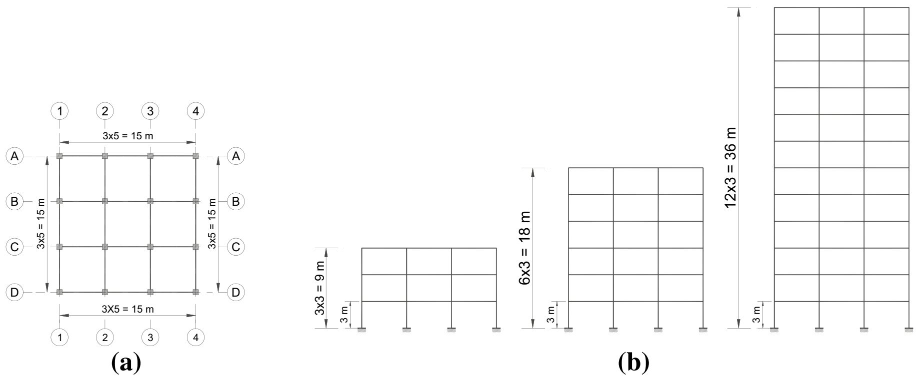

Fig. 4 Three-, six- and twelve-story buildings: **a** typical floor plan, **b** elevation

Table 2 Cross-sections and rebar for column of the studied buildings

Building	Column position	Story no.							
		From 1 to 3		From 4 to 6		From 7 to 9		From 10 to 12	
		Size Rebar	ρ_s(%)	Size Rebar	ρ_s(%)	Size Rebar	ρ_s(%)	Size Rebar	ρ_s(%)
12-Story	Corner	60×60 24T22	2.53	50×50 20T20	2.51	50×50 20T16	1.60	40×40 20T16	2.50
	Edge	70×70 24T22	1.86	60×60 20T22	2.11	50×50 20T20	2.51	40×40 20T16	2.50
	Internal	80×80 28T25	2.15	70×70 28T22	2.17	60×60 24T22	2.53	50×50 20T22	3.04
6-Story	Corner	50×50 20T16	1.60	40×40 20T16	2.50				
	Edge	50×50 20T20	2.51	40×40 20T16	2.50				
	Internal	60×60 24T22	2.53	50×50 20T22	3.04				
3-Story	Corner	40×40 20T16	2.50						
	Edge	40×40 20T16	2.50						
	Internal	50×50 20T20	2.51						

ρ_s% is the reinforcement ratio to the concrete section area

2.4 Building finite element modelling

The seismic pounding among three aligned adjacent RC-MRF buildings with three-, six- and twelve-stories during seismic events is investigated. A three-dimensional finite element (3D FE) model has been defined and nonlinear time-history analyses have been performed. The 3D FE models of the studied buildings are adopted to consider the significance of the accidental torsion requirement in Section 12.8.4.2 of ASCE 7-10 for buildings. The accidental torsion provisions require application of 5% offset of the centre of mass in each of two orthogonal directions to compute a torsional moment, thus increasing the base shear seismic design demands. The finite element software ETABS (CSI 2013, 2016) has been used to perform the dynamic analysis utilizing a set of nine-ground motion records to excite the buildings models. Rayleigh damping of 5% damping ratio is adopted, the coefficients multiplying the mass and stiffness matrices are calculated based on carefully selected frequencies of the studied buildings. The total seismic mass is calculated as dead load plus an additional 25% of live load based on the ASCE7-210 in Section 12.7.2 for the effective seismic weight of the building used for seismic based shear calculation. The practice on buildings subjected to earthquakes shows that masonry infill walls completely modify the behaviour of bare frames due to increased initial stiffness and low deformability, but it is difficult to predict the masonry infill effect on the frames members, as different failure modes can occur either in the masonry or in the surrounding frame. Thus, due to several uncertainties regarding the infill layout as non-structural elements, openings through infill wall, complications in modelling infill wall-frame interaction, the infill effects are hard to be quantified and usually ignored in structural design (Karayannis and Favvata 2005; Elwardany et al. 2017; Abdel Raheem et al. 2018a).

2.5 Structural impact model

To simulating pounding force between adjacent buildings, the gaps between the buildings are modelled by using compression only gap element as shown in Fig. 5. A linear damper is introduced to overcome the drawback of the linear viscoelastic model to simulate the energy dissipation (Komodromos et al. 2007; Polycarpou and Komodromos 2010; Jankowski 2010). The pounding force of impact model F_I is determined as:

$$F_I = \begin{cases} k\delta + c\dot{\delta} & \delta \geq G \\ 0 & \delta < G \end{cases} \quad \delta = u_i - u_j - G, \dot{\delta} = \dot{u}_i - \dot{u}_j \tag{2}$$

where δ and $\dot{\delta}$ define the relative displacement and velocity between colliding structural elements. k and c are the stiffness and damping for the impact model, respectively. u_i, u_j and $\dot{u}_i, \dot{u}_j$ are the displacement and velocity of the element's nodes i, j and G is the separation gap.

Numerous researches have been scrutinized the different possibilities for determination of the gap element stiffness. Watanabe and Kawashima (2004) have performed a numerical simulation to lighten the suitable stiffness of impact spring and the time interval of numerical integration based on the wave propagation theory, it concluded that the impact stiffness can be defined as the axial stiffness of the contact bodies, a gap element with stiffness equal to the axial stiffness of floor at the impact level is integrated (Maison and Kasai 1992). Anagnostopoulos (1988) proposed gap element with twenty times amplification factor multiplied with the lateral stiffness of the stiff SDOF system. In current study, the impact stiffness of the gap element k is determined as the greater value of either the axial stiffness of the collided floors or the lateral stiffness of the stiffer building at the impact level (Kawashima and Shoji 2000; Abdel Raheem 2009; Guo et al. 2012).

$$k = \gamma \frac{EA}{b} \quad or \quad \gamma \frac{3EI}{h^3} \tag{3}$$

where, A is the area of the impact surface, E is the modulus of elasticity, and b is building width in the impact direction, I is the moment of inertia of equivalent cantilever model of the stiffer building, h is the height building up to the impact level. A sensitivity analysis is done for the selection of the value of impact stiffness; on which the stiffness amplification factor is determined, $\gamma = 50$. Energy dissipation during contact is accounted through damping constant c. Insensitivity of displacement response to spring stiffness has also

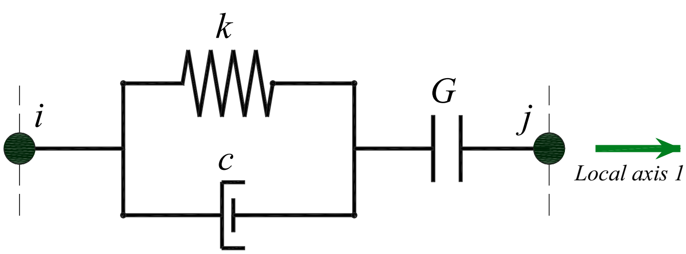

Fig. 5 Viscoelastic impact model

been reported by others (Anagnostopoulos 1988; Maison and Kasai 1992). However, the acceleration response may be strongly influenced by overly large values of spring stiffness and may compromise the accuracy of the model dynamic response. The damping component is used in the impact element to account for the amount of energy dissipation during each pounding. Reasonable values of this coefficient can be determined by relating it to the coefficient of restitution, e, for two masses, m1 and m2, colliding with arbitrary velocities (Anagnostopoulos 1988)

$$c = 2\xi\sqrt{k\frac{m_1 m_2}{m_1 + m_2}} \quad \text{and} \quad \xi = \frac{-\ln e}{\sqrt{\pi^2 + (\ln e)^2}} \tag{4}$$

The coefficient of restitution ranges between 0 and 1, which represents completely plastic impact to elastic impacts, respectively. A coefficient of restitution of 0.65 ($\xi = 0.14$) has been used for building collisions involving concrete-to-concrete impacts (Anagnostopoulos 1988; Jankowski 2006; Shakya et al. 2008).

3 Required gap separation to avoid pounding

The minimum code-specified separation of adjacent buildings (ICBO 1997) necessitates that all structures be detached from neighbouring structures. Separation should take into consideration the maximum inelastic displacement response Δ_M, where $\Delta_M = 0.7R\ \Delta_S$, in which R is the numerical coefficient that considers the inherent over-strength and global ductility capacity of lateral force resisting systems and Δ_S is the design level of displacement response under the design seismic forces. Seismic codes provisions and design regulations worldwide state minimum separation distances to be implemented among adjacent buildings, to prevent pounding, which is clearly equal to the relative displacement demand of the two conceivably colliding structural systems (ICBO 1997; ICC 2009; Garcia 2004). The minimum separation distance could be given by either ABSolute sum (ABS) or Square Root of Sum of Squares (SRSS) or Double Difference Combination (DDC) as follow:

$$\text{ABS:} \quad \mathrm{S} = u_A + u_B \tag{5}$$

$$\text{SRSS:} \quad S = \sqrt{u_A^2 + u_B^2} \tag{6}$$

$$\text{DDC:} \quad S = \sqrt{u_A^2 + u_B^2 - \rho_{AB} u_A u_B} \tag{7}$$

where S is the separation distance, u_A, u_B are the peaks of the displacement time history responses of adjacent buildings A and B at the impact level, respectively. ρ_{AB} is the correlation coefficient that depends on the damping and period ratio of the adjacent buildings. The ABS and SRSS rules provide unreasonably conservative separation distances that are extremely hard to be successfully executed, particularly when the adjacent structures have close matching vibration characteristics. The Double Difference Combination (DDC) rule is a more sound approach for evaluation of the critical required separation, which is almost equivalent to the peak relative displacement response (Jeng et al. 1992; DesRoches and Muthukumar 2002). Three various criteria to estimate the separation required to avoid seismic pounding between structural systems were inspected. None of the criteria assessed is completely perfect as in none of them gives separations that are reliably corrector somewhat conservative. The code-prescribed width of the separation joint could be insufficient when the fundamental periods of the adjacent buildings are close to the excitation frequency due to resonance phenomenon. Observations indicate that there is still a need to adequately characterize the correlation between displacement responses of nonlinear systems (Abdel Raheem 2014). The relative separation demand u_{Rel} that is calculated as the peak of the relative displacement time history response of adjacent buildings is a more realistic approach. The pounding risk of adjacent buildings is significantly affected by the natural period of an individual building, the period ratio and height ratio of adjacent buildings and the frequency content of the input excitation. The methods used in different codes provide poor estimates of the required building separation due to improper treatment of the vibration phase of adjacent buildings.

4 Numerical results and discussion

Three MRF buildings, 3-storey, 6-story and 12-storey buildings are aligned together to produce three different configurations (I, II, III) of adjacent buildings in series. These configurations of buildings are subjected to nine strong ground motions that are absolutely compatible with the design spectrum. Various parameters are investigated such as natural vibration, minimum required separation gap; displacement and acceleration response demands, and story shear force demands. The inelastic time-history responses of these RC MRF buildings are evaluated by means of the structural analysis software ETABS (CSI 2016). Comprehensive analysis of the response results is employed to draw significant conclusions. In crowded cities, building structures are usually constructed in close proximity to one another because of restricted availability of space, gap size G = 0, which has to do with structures in contact (lower limit of gap). In addition, three gap size of 2 cm, 6 cm, 12 cm are scrutinised. The nonlinear dynamic time history analysis for three different alignment configurations of adjacent buildings in series has been studied as shown in Fig. 6: (a) Configuration I (12-6-3), (b) Configuration II (3-12-6) and (c) Configuration III (6-3-12).

4.1 Natural vibration analysis

The determination of the vibration characteristics of a building can be obtained by experimental methods with observation of the dynamic in situ behaviour of the structure or using analytical modelling based on the mechanical properties of the components, including all elements contributing either to the mass or stiffness of the system. The vibration characteristics for the studied adjacent buildings in terms of fundamental period and vibration modes as gained from the structural analysis using finite element models and empirical expression in the ECP-201 and other international building codes (ICBO 1997; ICC 2009; ECS 2004; NRCC 2005; ECP 2008) are listed in Table 3.

In most structural design, empirical building period formulas are used to initiate the design process (Kwon and Kim 2010). The vibration periods and modal direction factor as dominated from the structural analysis using analytical models are indicated in Table 3; in addition, the fundamental period of vibration based on empirical equations in different international codes are introduced. The computed periods from empirical expressions are significantly shorter than those computed from structural models. The fundamental periods

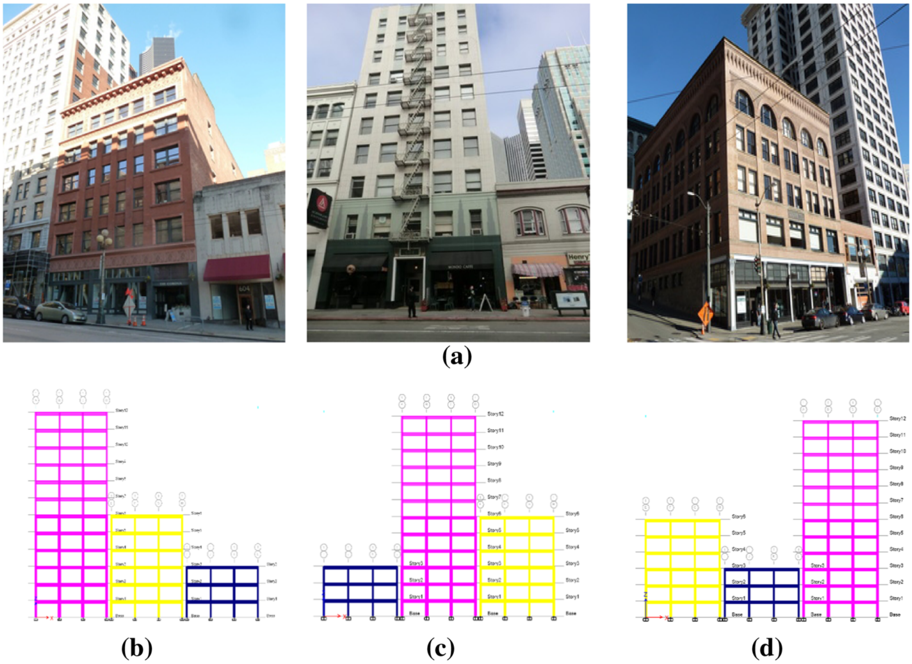

Fig. 6 Buildings system alignment configurations. **a** Potential pounding between adjacent buildings of different height without seismic gap (Openquake 2018), **b** configuration I (12-6-3), **c** configuration II (3-12-6), **d** configuration III (6-3-12)

Table 3 Free vibration characteristics of RC-MRF buildings

Design code	Period, T	Fundamental period (s)		
		12-Story	6-Story	3-Story
3D FE model vibration analysis	1st lateral vibration mode	1.566	0.897	0.533
	Torsional Vibration mode	1.369/0.522	0.820	0.503
	2nd lateral vibration mode	0.577	0.314	0.178
	3rd lateral vibration mode	0.335	0.184	0.113
ECP-201 (ECP 2008)	$T=0.075H^{3/4}$	1.102	0.655	0.390
ECP-201 (ECP 1993)	$T=0.1$ N	1.200	0.600	0.300
IBC (ICC 2009)	$T=0.073$ $H^{3/4}$	1.073	0.638	0.379
ICBO (ICBO 1997)	$T=0.049$ $H^{3/4}$	0.720	0.428	0.255
EC8 (ECS 2004)	$T=0.075$ $H^{3/4}$	1.102	0.655	0.390
NBCC (NRCC 2005)	$T=0.05$ $H^{3/4}$	0.735	0.437	0.260

H = the building's height measured from the base; N = number of stories

of the three building models based on ECP-201 (2008) are 1.102, 0.655, 0.390 s, whereas the fundamental period based on FE approach are 1.566, 0.897, 0.533 s, which reaches 142, 137, 137% for 12-story, 6-story and 3-story buildings that introduced in the code provisions. Hence it is clear that for the particular types of buildings that were considered, the code formulas could not provide the fundamental periods with sufficient accuracy in the calculation of vibration period which is considered the main parameter for lateral force procedure.

4.2 Minimum required separation gap among adjacent buildings

The common provision of building codes recommends a minimum separation gap based on maximum lateral displacements of each building to prevent pounding among adjacent structures. Although building codes take care of this problem, building designers are often reluctant to implement the required separation between buildings to eliminate pounding. To accomplish an adequately safe structural functioning throughout seismic hazards, an accurate seismic design should consider the relative displacements estimated using a non-linear time history analysis. The peak value of displacement time history responses of the no-pounding case for 12-story, 6-story and 3-story buildings (u_{12}, u_6, u_3) are listed in Tables 4, 5 and 6. The peak value determines the maximum displacement for standalone building at the potential level of impact with adjacent buildings. The peak response values are required to determine the required separation gap based on different codes using ABS, SRSS, and DDC rules. In addition, the critical separation distance, u_{Rel} is calculated as the peak value of the relative displacement time history response of all possible alignment configurations of adjacent three buildings in series "3-configurations I, II, III" under various input excitations.

Since the absolute sum (ABS) method considers complete out-of-phase response of the adjacent buildings, the ratio of u_{Rel} to the sum of u_A and u_B could be considered as a degree of out-of-phase of adjacent buildings, which depends on adjacent building vibration and input earthquake excitation characteristics. The out-of-phase displacement among buildings is obviously detected because of different vibration periods of the adjacent buildings. The closing and opening peak displacements are important to decide the level of prejudiced response of the pounding system. Thus, seismic pounding between adjacent buildings may cause unseemly damages albeit every standalone structure might have been designed perfectly to resist the hit of realistic earthquake actions.

Table 4 Peak values of the relative displacement between 12-story and 6-story models at 6th level of impact

Earthquake	u_{12} (m)	u_6 (m)	$u_{Rel_{12\&6}}$ (m)	$\frac{u_{Rel}}{\max(u_{12}\ or\ u_6)}$	$\frac{u_{Rel}}{u_{12}+u_6}$
San Simeon	0.079	0.115	0.144	1.246	0.739
Morgan Hill	0.077	0.141	0.165	1.170	0.755
Christchurch	0.109	0.122	0.162	1.335	0.703
L'Aquila	0.092	0.131	0.163	1.248	0.733
Loma	0.085	0.152	0.180	1.184	0.757
Imperial Valley-06	0.092	0.147	0.211	1.438	0.885
Bam	0.101	0.122	0.168	1.378	0.754
Kobe	0.090	0.171	0.227	1.327	0.870
Chi-Chi	0.107	0.148	0.168	1.130	0.657
Maximum	0.109	0.171	0.227	1.438	0.885
Average	0.093	0.139	0.176	1.273	0.761
Standard deviation	0.011	0.018	0.026	0.103	0.073

Table 5 Peak values of the displacements for 12-story and 3-story models at 3rd level of impact

Earthquake	u_{12} (m)	u_3 (m)	$u_{Rel_{12\&3}}$ (m)	$\frac{u_{Rel}}{\max(u_{12}\ or\ u_3)}$	$\frac{u_{Rel}}{u_{12}+u_3}$
San Simeon	0.033	0.077	0.076	0.983	0.687
Morgan Hill	0.032	0.077	0.056	0.738	0.519
Christchurch	0.045	0.082	0.081	0.983	0.636
L'Aquila	0.042	0.065	0.076	1.175	0.715
Loma	0.052	0.074	0.068	0.917	0.540
Imperial Valley-06	0.051	0.071	0.077	1.088	0.630
Bam	0.048	0.077	0.059	0.768	0.475
Kobe	0.046	0.064	0.085	1.315	0.764
Chi-Chi	0.055	0.075	0.066	0.889	0.512
Maximum	0.055	0.082	0.085	1.315	0.764
Average	0.045	0.073	0.072	0.984	0.609
Standard deviation	0.008	0.006	0.010	0.186	0.102

Table 6 Peak values of the relative displacements for 6-story and 3-story models at 3rd level of impact

Earthquake	u_6 (m)	u_3 (m)	$u_{Rel_{6\&3}}$ (m)	$\frac{u_{Rel}}{\max(u_6\ or\ u_3)}$	$\frac{u_{Rel}}{u_6+u_3}$
San Simeon	0.072	0.077	0.105	1.366	0.708
Morgan Hill	0.071	0.077	0.108	1.412	0.732
Christchurch	0.074	0.082	0.119	1.448	0.762
L'Aquila	0.075	0.065	0.091	1.219	0.653
Loma	0.083	0.074	0.104	1.246	0.661
Imperial Valley-06	0.070	0.071	0.112	1.587	0.796
Bam	0.071	0.077	0.099	1.274	0.665
Kobe	0.086	0.064	0.119	1.393	0.796
Chi-Chi	0.076	0.075	0.107	1.415	0.713
Maximum	0.086	0.082	0.119	1.587	0.796
Average	0.075	0.073	0.107	1.373	0.721
Standard deviation	0.006	0.006	0.009	0.114	0.056

The critical separation distance is calculated as the peak values of the relative displacement time history responses at all the potential pounding levels and all the possible potential alignment of the adjacent buildings. The required separation is calculated for the no-pounding case, where the interaction between adjacent buildings of all configurations due to pounding is neglected. The separation distance u_{Rel} obtained based on non-linear time history analysis is compared with the corresponding estimate that is based on ABS response combination rule suggested in the seismic design code. The average required separation distances at the potential level of impact reach 0.176 ± 0.026 m between 12-story and 6-story buildings; and 0.072 ± 0.010 m between 12-story and 3-story buildings; and 0.107 ± 0.009 m between 6-story and 3-story buildings. While the maximum required separation distance could reach 0.227, 0.085, 0.119 m with ratio to the code defined minimum required gap distance 88, 76, and 80%, respectively. The ABS approach provides an over-conservative approach for determining the required separation distances to avoid seismic pounding between adjacent buildings.

4.3 Effect of separation gap size on seismic response demands

The nonlinear dynamic analyses have been carried for four different gap sizes; G = 2, 6 and 12 in addition to in-contact adjacent buildings, G = 0. The magnification in response demands of adjacent buildings depends on natural vibration period of each building and their ratio besides the dominant frequency of input excitation. In addition to the height ration and alignment configuration of adjacent buildings whether the building is an exterior or interior in the buildings alignment, hence the building is exposed to one- or two-sided impacts. Table 7 presents the peak displacement responses at pounding levels for configuration II under different earthquakes and compared to no pounding case. For left exterior 3-story building and right exterior 6-story building, pounding with one-side impact reduces the peak displacement response demand of building in both impact and rebound directions, where the peak responses in the impact direction are significantly decreased about 50–75% and 38–56% of that no-pounding case, the peak responses in the rebound direction are slightly decreased with 10% and 20% at maximum of that no-pounding case for 3-story and 6-story buildings, respectively. For the interior 12-Story building with two sided-impacts at 3rd and 6th levels, the displacement response demand decreases due to pounding in the impact direction at both 3rd and 6th levels with 15% at maximum of that no-pounding case, while the displacement response demand increases in the rebound direction at 6th story level with maximum 17% of that no-pounding case, and at 3rd level, the rebound displacement could be increased 7% or decreased 20% depending on the input excitation.

Figure 7 presents the displacement mean and maximum responses envelops for different spacing sizes that confirms the trend of impact effect on the displacement response demands of the adjacent building in configuration II of buildings alignment. The peak of story displacement response depends on the input excitation characteristics and gap size, enlarging separation gap width is most likely effective to eliminate contact when

Table 7 Peak displacement response (m) at pounding level (configuration II, G = 0)

Earthquake response	Impact between 3- and 12-story buildings				Impact between 12- and 6-story buildings			
	3-Story building		12-Story building				6-Story building	
	3rd level				6th level			
	Rebound	Impact direction		Rebound	Rebound	Impact direction		Rebound
Kobe								
No pounding	−0.059	0.064	−0.046	0.046	−0.089	0.090	−0.171	0.156
Pounding	−0.058	0.032	−0.043	0.037	−0.093	0.078	−0.078	0.128
%	−2	−50	−7	−20	4	−13	−54	−18
L'Aquila								
No pounding	−0.065	0.061	−0.040	0.042	−0.084	0.092	−0.131	0.105
Pounding	−0.063	0.027	−0.035	0.045	−0.098	0.093	−0.057	0.092
%	−3	−56	−13	7	17	1	−56	−12
San Simeon								
No pounding	−0.057	0.077	−0.033	0.030	−0.079	0.072	−0.113	0.115
Pounding	−0.052	0.019	−0.033	0.027	−0.086	0.061	−0.070	0.092
%	−9	−75	0	−10	9	−15	−38	−20

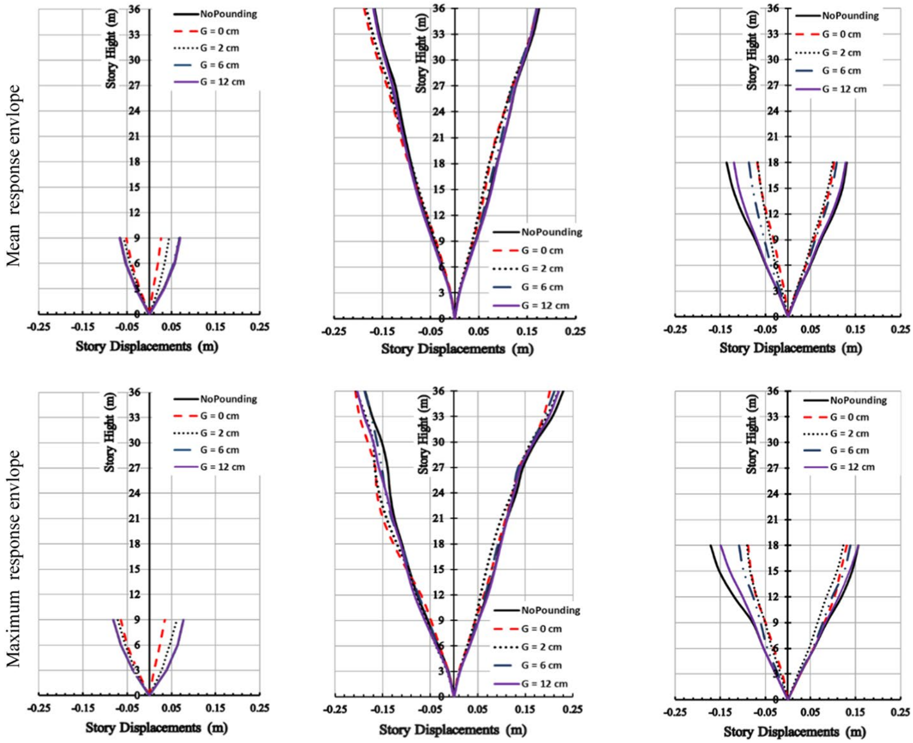

Fig. 7 Displacement mean and maximum responses envelops for different spacing sizes (configuration II)

the separation is adequately wide. A gap size of 6 cm is sufficient to significantly reduce the impact effect between 3- and 12-story adjacent buildings, while a gap size of more than 12 cm is required to significantly reduce the impact effect at 6th level between 6- and 12-story adjacent buildings. The seismic pounding provides displacement restrains on the impacting side, but may amplify displacement responses on the other side, particularly the response of 12-story building at the height levels above the impact level. Furthermore, the maximum responses in the short building are decreased in the impact and rebound directions. It can be concluded that in the shorter building pounding results in reduction of displacements in all stories while in the taller building generally the response decreases in the lower levels but only slightly increases in the upper ones. The pounding effect of the impact at the 6th level is more significant than that of impact at 3rd level.

Table 8 presents the peak acceleration responses at pounding levels for configuration II under different earthquakes and compared to no pounding case. Exterior buildings at end of adjacent buildings alignment are exposed to one-sided impacts and as a rule experience, the acceleration response magnification in the rebound direction can be very significant and could reach 360% at the top of the 3-story building, 654% at the top of the 6-story building. Interior buildings, in contrast, are exposed to two-sided impacts that can cause significant amplifications of acceleration response at the impact level that could reach 450% and 547% at 3rd and 6th level of impact, respectively. The peak acceleration responses depend on separation gap size and input excitation characteristic.

Table 8 Peak acceleration response at pounding level (configuration II) (m/s^2)

Earthquake response	Impact between 3- and 12-story buildings				Impact between 12- and 6-story buildings			
	3-Story building		12-Story building				6-Story building	
	3rd level				6th level			
	Rebound	Impact direction		Rebound	Rebound	Impact direction		Rebound
Kobe								
No pounding	−9.56	9.73	−7.29	6.35	−7.34	7.10	−12.53	10.83
Pounding G=0	−26.14	10.27	−26.83	22.00	−36.08	15.51	−9.74	50.90
Pounding G=2	−32.12	11.67	−22.33	28.56	−36.06	17.89	−10.66	46.61
L'Aquila								
No pounding	−10.34	8.95	−8.36	7.46	−8.92	8.35	−10.17	11.24
Pounding G=0	−37.25	11.07	−20.48	33.19	−45.39	20.34	−9.09	56.87
Pounding G=2	−16.15	9.77	−32.71	20.26	−38.90	18.50	−9.25	43.97
San Simeon								
No pounding	−9.43	11.07	−6.24	5.97	−6.98	7.60	−9.01	9.26
Pounding G=0	−27.51	9.54	−22.58	23.17	−37.60	26.81	−9.70	55.87
Pounding G=2	−30.24	11.38	−22.78	15.13	−38.15	28.28	−10.50	60.60

Figure 8 presents the acceleration response time histories of the colliding buildings at the potential top level of the 6-story and 3-story buildings for different gap sizes, under San Simeon earthquake record. The acceleration response is amplified due to collision among the adjacent buildings and can gain several times that from no-pounding case. The most evident change in the graphs is that there are upsurges in negative accelerations for 3-Story

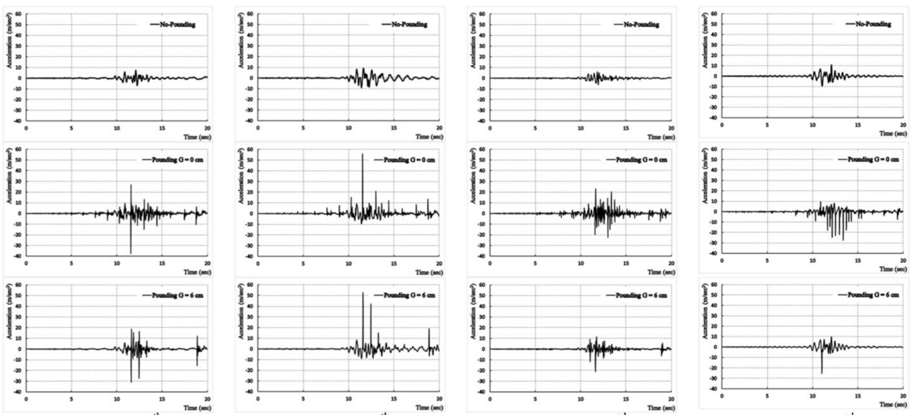

12-Story building (6th level) 6-Story building (6th level) 12-Story building (3rd level) 3-Story building (3rd level)

Fig. 8 Acceleration time histories under the San Simeon earthquake for different gap size (configuration II) building and in positive accelerations for 6-Story building due to the configuration arrangement, while for 12-Story building the increase occur in positive and negative accelerations. For G = 0 cm, the peak negative acceleration at top level of 3-story building is as high as -27.51 m/s^2 at 13.38 s. It is nearly three times greater related to no pounding acceleration which is only -9.43 m/s^2 at 11.07 s. The peak positive acceleration produced in 6-story building during collision is as much as 55.87 m/s^2 at 11.55 s. It is about six times greater than the peak acceleration for no pounding case which is only 9.26 m/s^2 at 11.65 s. While for 12-story building, the crowning negative acceleration at 6th level (critical pounding level) is as high as -37.6 m/s^2 at 11.53 s. It is 5.4 times higher related to no pounding acceleration which is only -6.98 m/s^2 at 12.26 s, and the greatest positive acceleration at 3rd level is as high as 23.17 m/s^2 at 11.65 s. It is 3.9 times higher related to no pounding acceleration which is only 5.97 m/s^2 at 11.85 s. The time lag of the impact of the interior building with the right and left exterior buildings and different levels of impact reduce the impact interaction effect on the response demands of adjacent buildings in series, Synchronized impact at different levels of impact could maximize the adjacent building interaction and impact effects.

Considering that losses due to non-structural components have consistently been reported to be far greater than those resulting from structural damage, it is imperative to consider maximum story horizontal accelerations. Modern code design provisions evaluate the maximum story horizontal accelerations to design the non-structural systems and their connections to the main structure. Nevertheless, the pounding phenomenon between adjacent buildings is not taken into account, which generally leads to higher values of the accelerations in comparison with the case of well-separated buildings. This characteristic can be observed in Fig. 9, which depicts the story horizontal acceleration envelopes for buildings in contact with different gap sizes and no-pounding case. The figure comprises that results that examines mean and maximum responses for nine input excitations and response under Loma earthquake. It is evident that buildings subjected to pounding generally present higher story acceleration in comparison with no pounding case. Therefore, it is obvious that the maximum story horizontal accelerations of buildings are strongly affected by the seismic gap between the collided buildings. The acceleration response of high-rise building at the height levels below the impact levels is significantly amplified at both directions due to two-sided impact, the response gets its maximum values at pounding of in-contact building and with small gap size of 2 cm and decrease effectively with the increase of gap size, while the response of the floors at the height levels above the impact level is slightly affected. Furthermore, the maximum responses in the low rise building are significantly increased in the rebound directions over the whole height of building, while the response in the impact direction is slightly affected due to one-side impact for the exterior building of adjacent in series alignment buildings.

Figure 10 presents the story shear mean and maximum responses envelops for different spacing sizes, the figure comprises results that examine the mean and maximum responses for nine input excitations and selected response under Chi-chi earthquake. It is evident that buildings subjected to pounding are strongly affected by the seismic gap between the collided buildings. The story shear response of 12-story building at the height levels above the impact levels is significantly amplified at the rebound direction due to two-sided impact, the response gets its maximum values at pounding of in-contact building and with small gap size of 2 cm and decrease effectively with the increase of gap size, while the response of the floors at the height levels below the impact level is slightly affected. The sway of the higher building is suddenly limited by the shorter building and it experiences high story

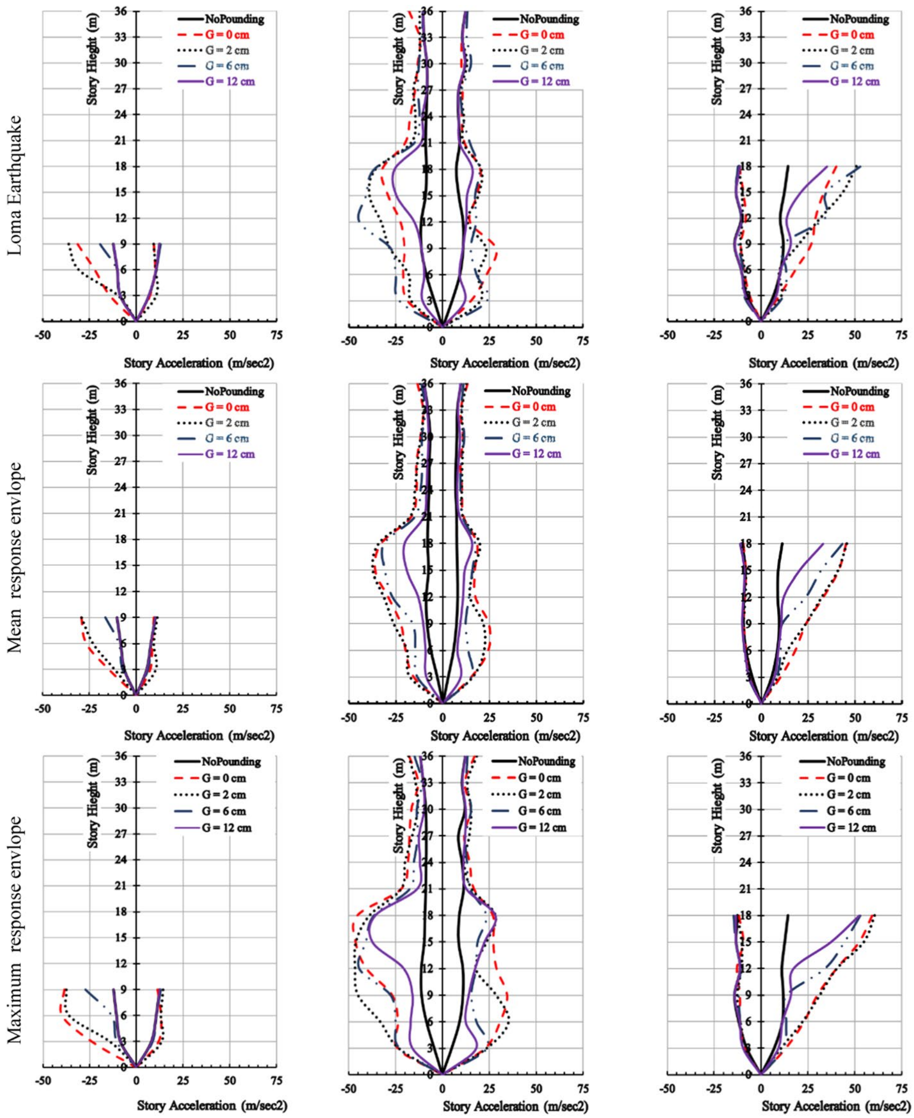

Fig. 9 Acceleration mean and maximum responses envelops for different spacing sizes (configuration II)

shear forces above the pounding level. For the 12-story interior building, the 12-story and 3-story impact leads to an increase in the story shear response along the height above the 3rd level in the rebound direction relative to the collided buildings. Moreover, the 12-story and 6-story impact leads to an increase in the story shear response along the height above the 6th level in the rebound direction relative to the collided building. Furthermore, the maximum responses in the exterior 3- and 6-story low rise buildings are significantly decreased in both directions over the whole height of building. Moreover, the response in the impact direction is slightly affected due to one-side impact for the exterior building of

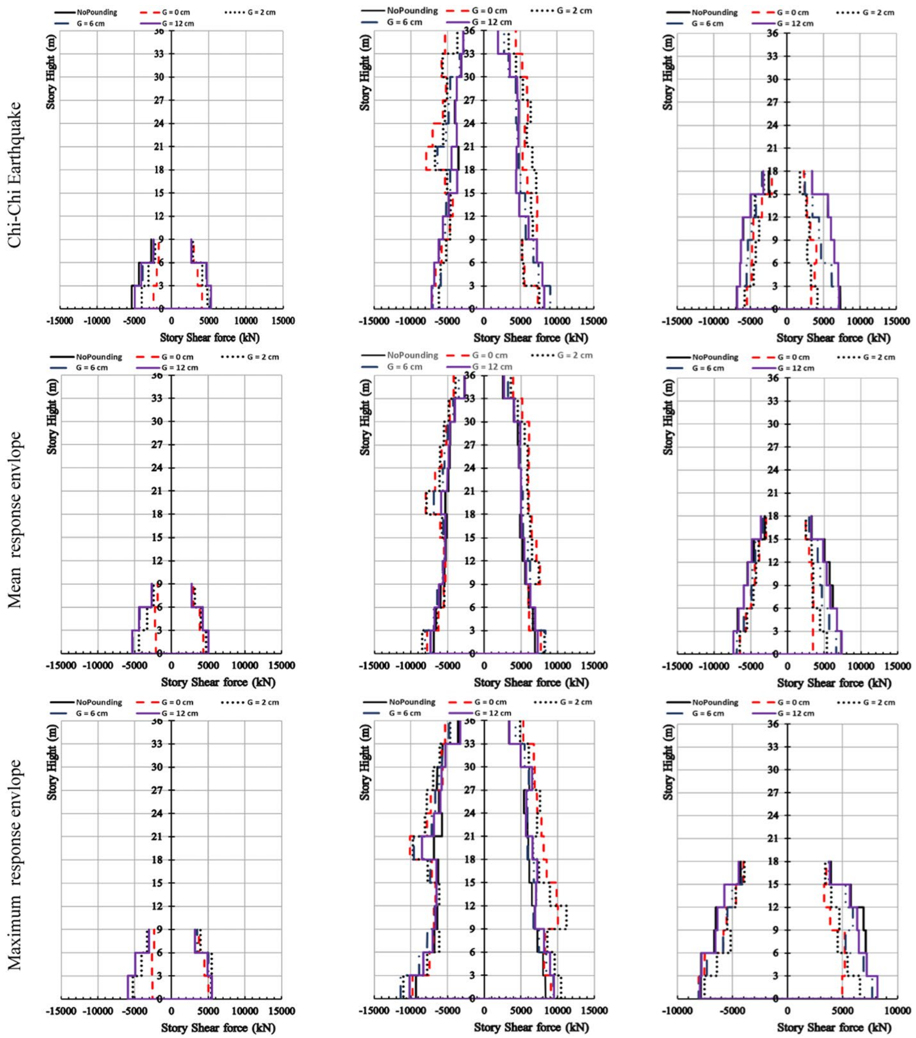

Fig. 10 Story shear mean and maximum responses envelops for different spacing sizes (configuration II)

in series alignment buildings. The amplification of shear force response is more significant in the higher adjacent building. The height ratio of the adjacent buildings has significant role on the pounding effects compared to vibration period ratio. Due to pounding, the maximum variation in shear forces of the higher building is always observed in the storey above the top floor of the shorter adjacent building. This floor is always the location of the first probable collision between the adjacent buildings. Pounding has a considerable effect on the story shear response of the higher building in the stories upper than roof of the shorter structure. It is observed that pounding can make the story shear in the stories just higher than roof of the shorter building to surpass those of the lower ones.

Table 9 presents the peak story shear responses at impact levels and at base for configuration II under different earthquakes and compared to no pounding case. For the exterior buildings, the story shear response demands are significantly reduced up to 61% and 65%

Table 9 Peak story shear at pounding level (configuration II) (kN)

Earthquake response	Impact between 3- and 12-story buildings				Impact between 12- and 6-story buildings			
	3-Story building		12-Story building				6-Story building	
	At base level		3rd level	6th level	At base level		At base level	
	Max (+)	Max (−)	Max(+)	Max(−)	Max(+)	Max(−)	Max(+)	Max(−)
Kobe								
No pounding	4578	− 5303	5454	− 5927	7847	− 7274	7946	− 7810
Pounding G = 0	5041 (10%)	− 2589 (− 51%)	6892 (26%)	− 7971 (34%)	7987 (2%)	− 9509 (31%)	3751 (− 53%)	− 8084 (4%)
Pounding G = 2 cm	4590 (0.2%)	− 5252 (− 1%)	6795 (25%)	− 7573 (28%)	7942 (1%)	− 8047 (11%)	6408 (− 19%)	− 7034 (− 10%)
L'Aquila								
No pounding	5315	− 4597	5367	− 5910	6140	− 6770	7198	− 7281
Pounding G = 0	4902 (− 8%)	− 2429 (− 47%)	7556 (41%)	− 7243 (23%)	8119 (32%)	− 7728 (14%)	2832 (− 61%)	− 6959 (− 4%)
Pounding G = 2 cm	5307 (− 0.1%)	− 4294 (− 7%)	7131 (33%)	− 6669 (13%)	8512 (39%)	− 8845 (31%)	4084 (− 43%)	− 5326 (− 27%)
San Simeon								
No pounding	4621	− 5604	4596	− 3903	5127	− 5146	7643	− 6870
Pounding G = 0	4696 (2%)	− 1990 (− 64%)	6472 (41%)	− 10,112 (159%)	7273 (42%)	− 8357 (62%)	3162 (− 59%)	− 7119 (4%)
Pounding G = 2 cm	4128 (− 11%)	− 4341 (− 23%)	6852 (49%)	− 9711 (149%)	9256 (81%)	− 7717 (50%)	4936 (− 35%)	− 7342 (7%)

of that of no-pounding case for the 3- and 6-story buildings, respectively. For 3-story exterior building, the mean story shear responses are reduced up to 35% and 17%, while the maximum responses are reduced up to 16% and 23% for in-contact pounding (G = 0) and gap size of 2 cm. For 6-story exterior building, the mean story shear responses are reduced up to 32% and 35%, while the maximum responses are reduced up to 7% and 27% for in-contact pounding (G = 0) and gap size of 2 cm. While for the 12-story interior building, in contrast, is exposed to two-sided impacts that the story shear responses are significantly increased either at the base or just above the impact levels. The response magnification could reach 141%, 260% and 162% at the 3rd and 6th levels of impact and at base for in-contact pounding. Furthermore, with the increase of gape size, G = 2 cm, this effect could increase or decrease (149%, 249% and 181%) depending the input excitation. For 12-story interior building, the mean story shear responses at base level are increased up to 52% and 65%, while the maximum responses are increased up to 62% and 80% for in-contact pounding (G = 0) and gap size of 2 cm.

Table 10 presents peak pounding force induced under Chi-Chi earthquake for different gap sizes. The pounding between 3-story building and 12-story buildings at 3rd story level displays higher value of the impact force for gap size G = 2 cm, even greater than the case of in-contact alignment G = 0. Furthermore, the potential impact is extended over all stories for the in-contact case, with lighter impact at lower stories. The pounding between 6-story building and 12-story buildings at 6th story level displays higher value of the impact force for gap size G = 6 cm that is close the case of in-contact alignment G = 0, and higher than that of case for G = 2 cm. In general, it is noticed that for a range of the separation gap near

Table 10 Peak pounding force induced under Chi-Chi earthquake for different gap sizes (kN) (configuration II)

Story	Impact force between 3- and 12-story buildings				Impact force between 12- and 6-story buildings			
	G = 0 cm	G = 2 cm	G = 6 cm	G = 12 cm	G = 0 cm	G = 2 cm	G = 6 cm	G = 12 cm
Story 6	–	–	–	–	13,032	8425	12,130	10,425
Story 5	–	–	–	–	12,499	7542	9879	4723
Story 4	–	–	–	–	10,272	9631	6369	0
Story 3	8054	10,872	1642	0	6004	7911	0	0
Story 2	6136	5808	0	0	4832	2003	0	0
Story 1	3327	0	0	0	2007	0	0	0

the middle third of maximum relative displacement, the impact force is rapidly increasing and then slightly decreases with further reduction or increase in the separation. The ratio of the offered seismic gap to the maximum relative displacements between adjacent buildings for each earthquake input excitation appears to play an important role in the severity of the structural pounding and its consequences. Pounding may occur at different floor levels, allowing the activation of multiple contact locations along the height of the buildings.

Figure 11 shows the sequence of impact force and relative displacement time history responses at the top levels of the 6-story and 3-story buildings for different gap sizes (G = 0, 6 cm) under Kobe earthquake, since the top levels experience the most critical condition. For the relative displacement time history, positive values depict opening and rebound relative displacements, while negative values result from the event of impact causing the pounding. The occurring of pounding develops larger rebound displacements. The acceleration response variation at the impact level of the 6-story and 3-story buildings during collision between adjacent buildings in series under various earthquakes is determined. Pounding is a severe load condition that could result in unexpected magnitude and short duration acceleration spikes, which consecutively cause damage to building contents. An abrupt stopping of velocity at the impact level results in great and quick acceleration pulses in the opposite direction. The adjacent buildings tend to pound together in several different times if the separation gap gets narrower. Damage potential due to pounding not only governed by the magnitude of the collision force, but also by the recurrence number of strong impacts. Although the increase of separation gap from G = 0–2 to 6–12 cm develops larger

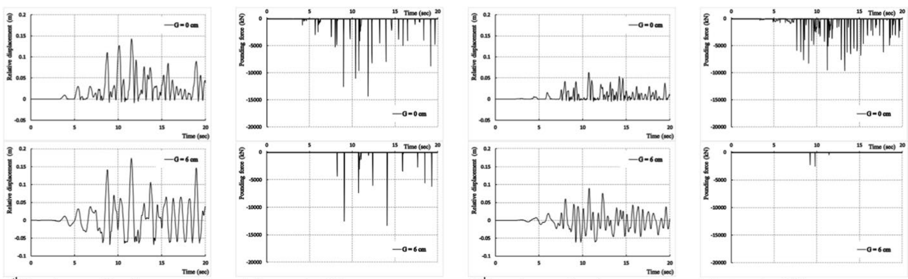

6th level pounding between 12- and 6-story buildings 3rd level pounding between 6- and 3-story buildings

Fig. 11 Displacement and pounding force response time histories under Kobe earthquake, configuration II opening relative displacements but in contrast it has the capability for decreasing impact effects and could decrease the number of pounding's event. Furthermore, enlarging separation gap width is most likely effective to eliminate contact when the separation is adequately wide. The pounding effect that primarily increases the story shear response is the de-acceleration that occurs when the adjacent buildings collide. However, the duration of the collisions is small. As pounding happens; the building experiences high impact forces and acceleration spikes at the instant of contact. The peak of acceleration response due to pounding could attain 10 times more than that of no-pounding case, which are within the range viewed in experimental results (Guo et al. 2009). Along the through-pounding floors, the displacements are reduced in the pounding side but increased in the no-pounding side and the story shears follow a similar pattern (Fig. 12).

4.4 Local damage due to pounding

The surveys on damage during past severe earthquakes show that pounding can lead to considerable damage or even collapse of buildings if the separation distance between them is not sufficient, the pounding usually caused local damage around the impacting areas. Building pounding can alter the basic response of the building to ground motion, and impart additional inertial loads and energy to the building from the adjacent structure. Of particular concern is the potential for extreme local damage to structural elements at the zones of impact. The energy balance analysis confirms that pounding, in addition to the local damage it usually causes, can increase or reduce the structural response, depending on the vibration characteristics of the adjacent buildings. A comparison between pounding and no-pounding cases indicates, however, that structural pounding may lead to a substantial increase of the range and intensity of damage. The results of the study show that collisions may lead to a significant increase of the response of the higher building as well as may result in a substantial increase of the range and intensity of damage at the base

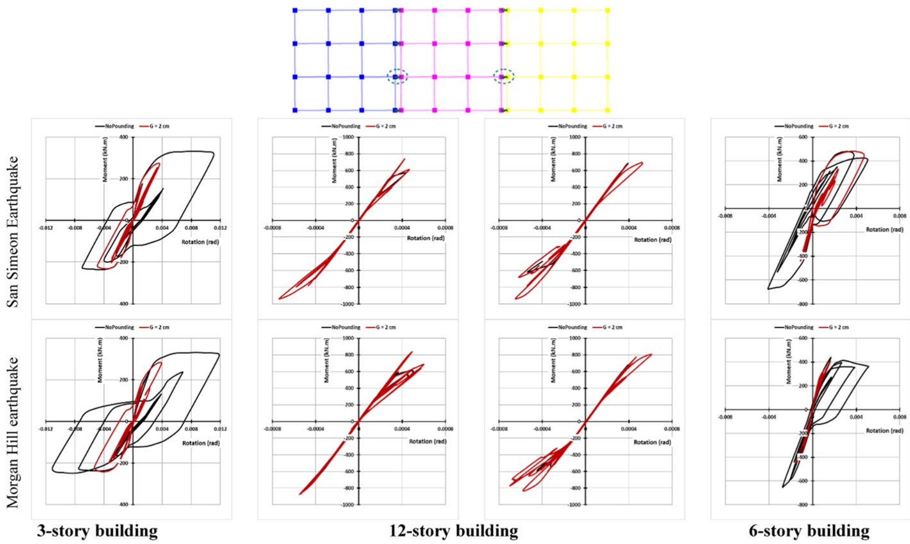

Fig. 12 Response cycles of the bottom plastic hinge of columns on the ground floor (configuration II)

of the structure. The results clearly confirm that for shorter adjacent buildings, the seismic vibrations reduced considerably; consequently, the severity of the probable pounding is reduced. As way of example of the hysteretic response of plastic hinges, the moment-rotation response cycles induced in the bottom end section of the most stressed column by two input motions are plotted in Fig. 13. It can be seen from the figure that the columns of the bottom storeys of the structure experience considerable inelastic behaviour at the bases. Furthermore, the gap values affect the corresponding local damage of beam. The higher adjacent building will be the most likely pounding damage to occur when earthquakes happen, larger lateral displacements and story shear of upper stories of the 12-story building should be behind the increase of damage in the same stories. The reduction of

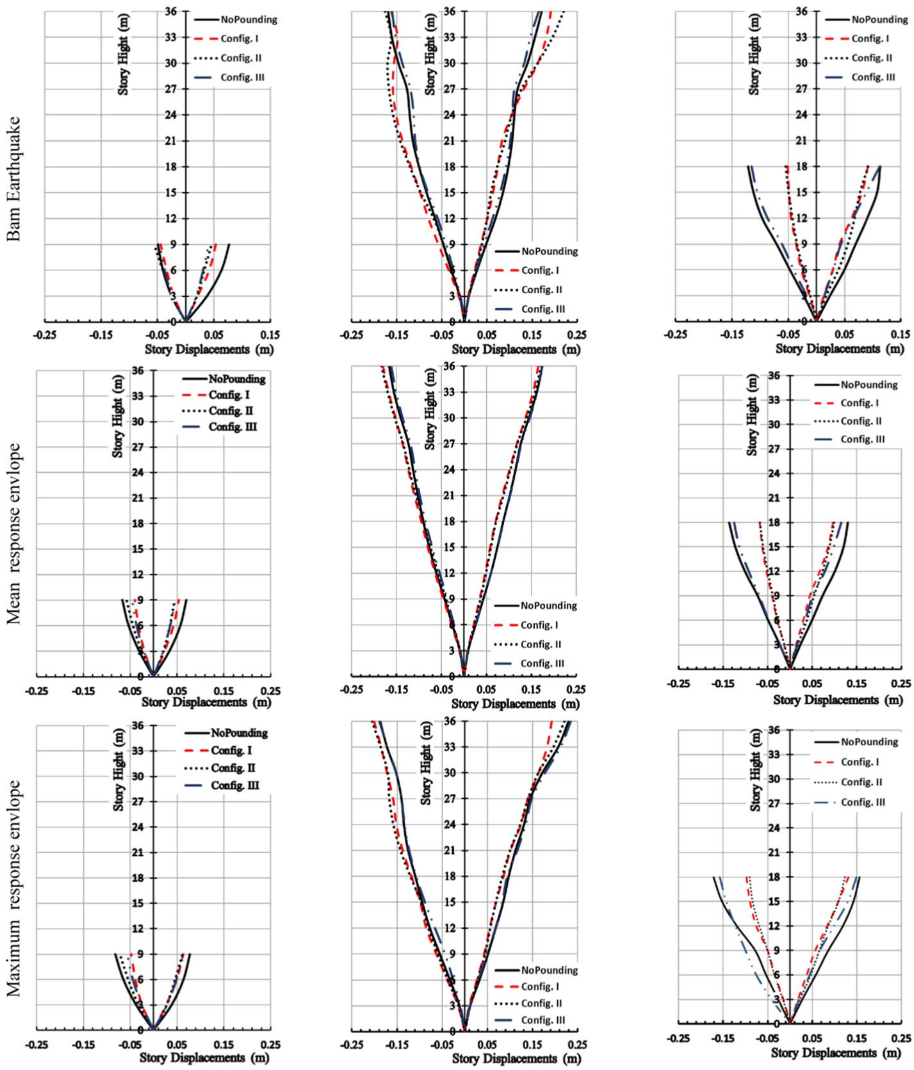

Fig. 13 Displacement mean and maximum responses envelops for different configurations (G = 2 cm)

seismic damage in beams, relative to no-pounding case, happens always in lower stories of both adjacent buildings along their common height. On the contrary, an increase of damage always is observed in the top stories of the shorter building and in the stories of the higher building on top of the roof of the shorter building. Table 11 presents maximum rotation of 0.013, 0.006 and 0.0008 radians for 3-, 6- and 12-story buildings for the no-pounding case. Furthermore, for pounding with gap size G = 2 cm, the rotation response decreases significantly for the shorter exterior buildings and reaches values of 0.011 and 0.047 for the 3- and 6-story buildings and slightly increased and reaches 0.0009 for the 12-story building. While for pounding with gap size G = 6 cm, the rotation response of the 3-story building doesn't change due to pounding, reach values of 0.048 for the 6-story buildings and slightly increased and reach 0.0012 for the 12-story building.

4.5 Effect of alignment configurations of the adjacent buildings

To evaluate the pounding effects on seismic response of buildings in series, interior and exterior building should be differentiated, the first exposed to two-sided impacts and the second to one-sided impacts. The magnification in the response buildings is extremely serious for cases with highly out-of-phase buildings. Two-sided pounding magnifies the stiff building response, and decreases the flexible building response. Due to pounding, the maximum variation in shear forces of the higher building is always monitored in the

Table 11 Rotation values at the bottom plastic hinge of columns on the ground floor (configuration II)

	3-Story building	12-Story building		6-Story building
San Simeon earthquake				
No pounding	0.0111	0.0004	0.0005	0.0051
Pounding G = 2 cm	0.0049	0.0007	0.0006	0.0047
Pounding G = 6 cm	0.0103	0.0008	0.0008	0.0035
Morgan earthquake				
No pounding	0.0118	0.0005	0.0004	0.0052
Pounding G = 2 cm	0.0053	0.0006	0.0007	0.0016
Pounding G = 6 cm	0.0118	0.0006	0.0007	0.0041
Christchurch earthquake				
No pounding	0.0131	0.0008	0.0009	0.0057
Pounding G = 2 cm	0.0057	0.0009	0.0008	0.0024
Pounding G = 6 cm	0.0131	0.0011	0.0012	0.0048
L'Aquila earthquake				
No pounding	0.0100	0.0008	0.0008	0.0050
Pounding G = 2 cm	0.0111	0.0008	0.0008	0.0018
Pounding G = 6 cm	0.0100	0.0008	0.0008	0.0046

story above the top floor of the shorter adjacent building. For shorter adjacent buildings, the seismic vibrations reduced considerably; consequently, the severity of the probable pounding is reduced. Figures 13, 14 and 15 show the response envelopes of adjacent buildings for different configurations under several earthquake records. The peak story displacement responses depend on the input excitation characteristics and alignment position of building in series. Comparing pounding-involved and independent vibration responses for the adjacent buildings in series for different configurations shows that the 12-story building is more influenced by pounding because it acts as a stopper for the external buildings. Although the 12-story has long period and higher amplitude of

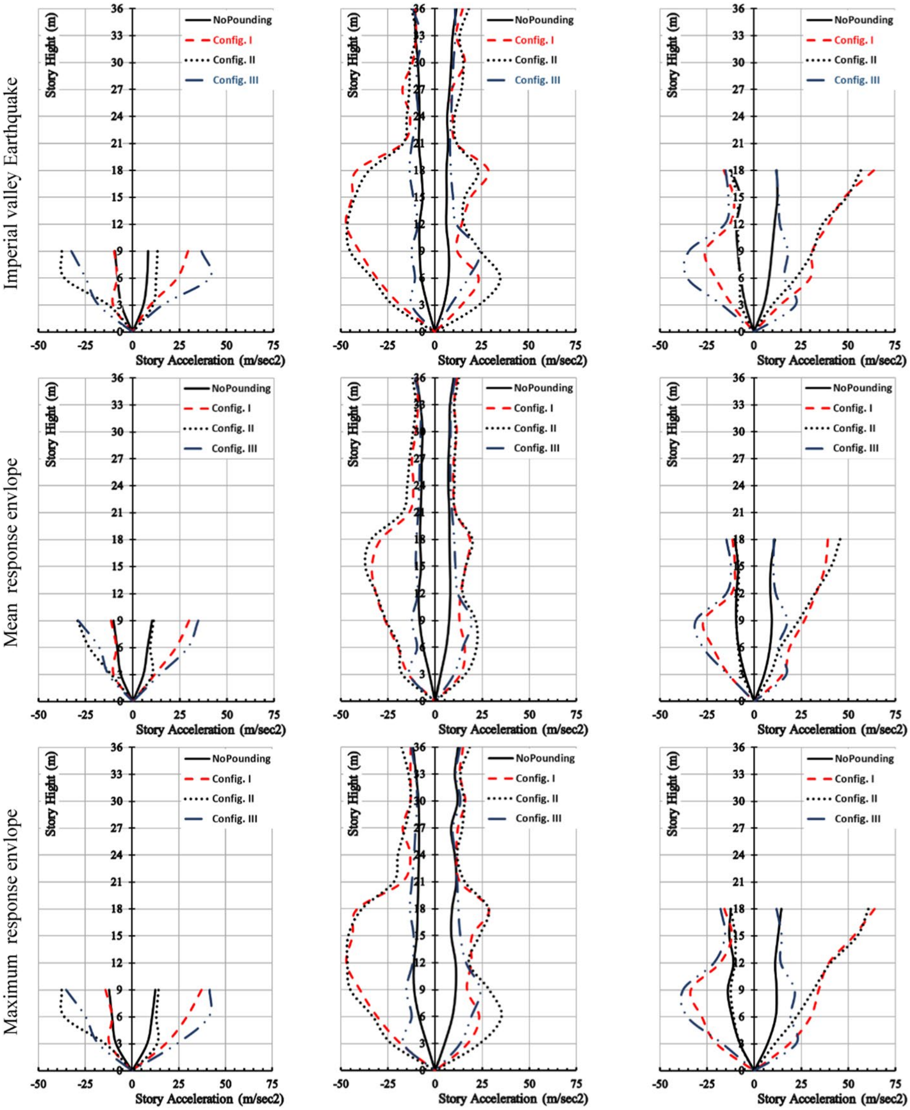

Fig. 14 Acceleration mean and maximum responses envelops for different configurations (G = 2 cm)

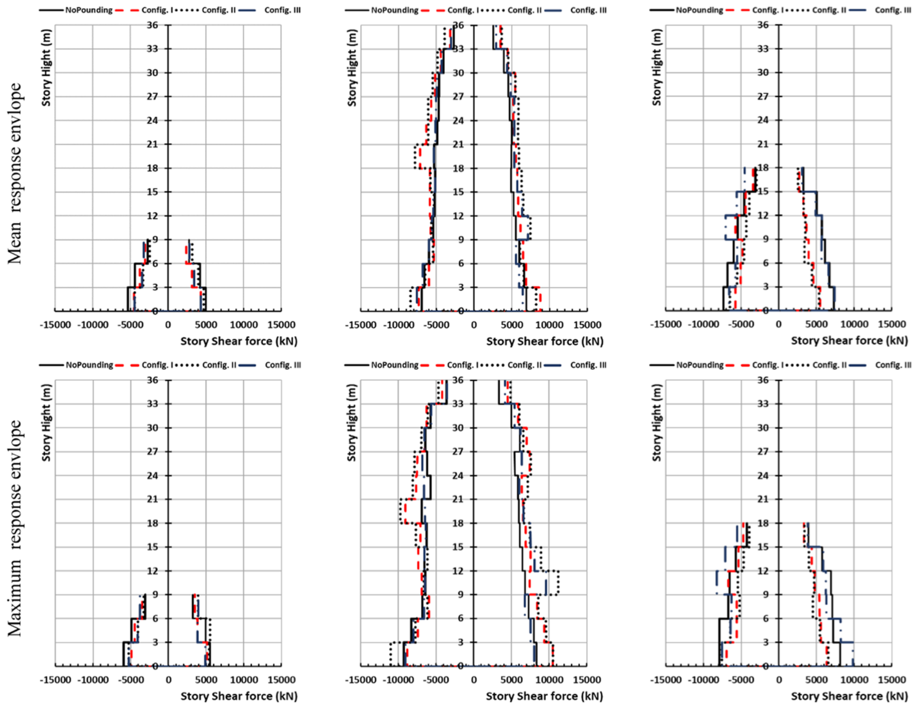

Fig. 15 Story shear mean and maximum responses envelops for different configurations (G = 2 cm)

motion and the 3- and 6-story shorter buildings have relative short periods, the 12-story building has relative high stiffens at the level of impacts. In configuration II, pounding has increased the peak absolute displacement of the middle high building above the impact level, as compared to the no pounding case. Whereas, it has decreased the peak displacement of the left and right relative short buildings.

Many of the buildings that survived after the earthquake have the benefit of being located between two buildings and behave as a unique building that has superior performance than those of the standalone building. The interior position of building among adjacent buildings reduces the potential damaging effects of the seismic pounding. As a short building is located between two high-rise buildings, the vibration amplitude of the short building is reduced and its effect on the two adjacent buildings is decreased as could be illustrated in configuration III (6-3-12). The displacement response demands are significantly reduced for 3-story interior building, slightly affected the response of the 6-story exterior building by increasing in the rebound direction and decreasing in the impact direction. While the response of 12-story building is almost not affected. In configuration I (12-6-3), the displacement response demands are significantly reduced for the 6-story interior building and the 3-story exterior short building, while the 12-story exterior high building has an increase of the response over the height above the impact level in the rebound direction, and response decreases in the impact direction. In configuration II (3-12-6), the displacement response demands are significantly reduced for the 3- and 6-story exterior buildings, while the 12-story interior high building has an increase of the response over the height above the impact level in the rebound direction, and response decreases in the impact direction, the impact effect is dominated by the impact with 6-story building.

In configuration I, pounding effect has decreased the mean and maximum peak displacement responses of the 6-story interior building and the 3-story exterior building by about 50, 44% and 35%, 34% as compared to the no pounding case, respectively. Whereas, the mean and maximum peak displacement responses of the 12-story exterior buildings could increase by about 11%, 14% in the rebound direction and decrease 22%, 19% in the impact direction. In configuration II, the mean and maximum peak displacement responses of the 12-story interior building increased by about 11 and 19% in the rebound direction and decrease 20 in the impact direction as compared to the no pounding case. Whereas, it has decreased the mean and maximum peak displacement responses of the left and right exterior buildings by about 38, 28 and 51%, 47% for 3-story and 6-story building, respectively.

An abrupt change of velocity direction at the impact level results in great and high acceleration pulses in the opposite direction. The acceleration response has high magnitude and short duration floor acceleration spikes, which in sequence cause foremost damage to building contents. In configuration III, a 3-story short building is located between two 6- and 12-story high-rise buildings, the vibration amplitude of the short building is decreased and acceleration response is increased and its influence on the 12-story adjacent building is negligible. The response of 6-story is significantly amplified below the impact level for the acceleration response, story shear above the impact level in the rebound direction. In configuration II, when a 12-story high-rise building is located between 3-story and 6-story buildings, its acceleration response is increased at the height levels below the collision level. At the levels over the collision level, no significant increase is observed in the responses. While, the mean and maximum acceleration responses of low rise building are slightly changes either increase or decrease in the impact direction and significantly increased in the rebound direction all over the building height. In configuration I, when a 6-story medium-rise building is located between 12-story and 6-story buildings, its acceleration response is increased at the height levels below the collision level. At the levels over the collision 3rd level, no significant change is observed in the responses compared to the no pounding case. While, the mean and maximum acceleration responses of 3-story low rise building are slightly changes either increase or decrease in the impact direction and significantly increased in the rebound direction all over the building height. The mean and maximum acceleration responses of 12-story building are slightly changes either increase or decrease above the impact level and significantly increased in the both directions below the impact level.

For the 12-Story building, pounding amplifies story shear response above impact level twice as much in configuration I, where it is in the left end of straight alignment as exterior building with one sided-pounding to 6-Story building. While in configuration II, the seismic responses of 12-story building as interior building with two sided-pounding are significantly increase for acceleration and shear force response demands. As the 12-Story building located in the right end as exterior building with one-sided pounding to 3-Story building in configuration III, the shear force response is not affected by pounding. The shear response of 6-Story building is increased by pounding in all configurations, but when it located in the right end, configuration II, the response amplification become less than other cases. The pounding has significant effects on the peak of story shear for 3-Story building as it has internal alignment and subjected to two-sided pounding. Seismic collision of 3-story buildings decreases the mean shear force demand over all stories below the collision level and improve the behaviour of structure for the different configuration either exterior with one-sided impact or interior with two-sided impact. However, in the case of 6-story buildings, story shear demands are decreased for the interior alignment in configuration I and exterior alignment in configuration II but the response is increased significantly, especially at the height level in which the collision is occurring (3rd level) and above for exterior alignment in configuration III. In the case of 12-story buildings, story shear demands are increased for the interior alignment in configuration II above the impact levels in the opposite direction of impact, and slightly affect below the impact levels. The response is increased significantly, especially at the height level in which the collision is occurring and above for exterior alignment in configurations I and III in rebounding direction. It is observed that the stiffer structure; 12-story building, irrespective of its relative alignment position, undergone the most story drift and shear force response magnification.

5 Conclusions

Seismic pounding is an extremely nonlinear phenomenon and a severe load case that could be a source of major structural damages. The present study scope focuses on the seismic pounding effects on response demands of adjacent buildings in series with equal story heights that predominantly affect the global and local response demands. The main importance of the current study stems from the emphasis on an accurate modelling of the seismic pounding between adjacent buildings in series; geometrically as well as in terms of material nonlinearity and more reliable and quantitative investigation of the problem that would lead to more practical results. The effect of collision is studied for different separation distances; three alignment configurations under nine ground motions, and then compared with no-pounding case. The local and global seismic performances of adjacent MRF buildings are scrutinized through numerical analyses. The global performance is examined through the maximum responses for the story displacement, acceleration and story shear seismic demands. Moreover, the responses for selected input excitation are presented to discuss the effect of the input excitation characteristics. While the local performances are examined through the accumulative energy and hysteresis for selected elements to characterize the nonlinear behaviour, in addition a comparison to that of no-pounding case are presented.

Based on the obtained results, it has been concluded that the severity of the pounding effects on the response of adjacent buildings in series depends on the vibration characteristics of the adjacent buildings, the input excitation characteristics, separation gap size, height ratio and the alignment position of the building in series: whether interior building with potential two-sided impacts or exterior building with potential one-sided pounding. It is noticed that for a range of the separation gap near the middle third of maximum relative displacement, the impact force is rapidly increasing and then slightly decreases with further reduction or increase in the separation. The ratio of the offered seismic gap to the maximum relative displacements between adjacent buildings for each earthquake input excitation appears to play an important role in the severity of the structural pounding and its consequences. Moreover, the pounding hazard of adjacent buildings could be amplified as the periods of buildings approach the dominant period of input excitation. Pounding may occur at different floor levels, allowing the activation of multiple contact locations along the height of the buildings. The vertical location of potential pounding extensively affects the distribution of story peak responses through the building height. It is observed that the stiffer structure; 12-story building, irrespective of its relative alignment position, undergone the most story drift and shear force responses magnification. The acceleration response of high-rise building at the height levels below the impact levels is significantly amplified at both directions due to two-sided impact, the response gets its maximum values at pounding of in-contact building and with small gap size of 2 cm and decrease effectively with the increase of gap size, while the response of the floors at the height levels above the impact level is slightly affected. Furthermore, the maximum responses in the low rise building are significantly increased in the rebound directions over the whole height of building, while the response in the impact direction is slightly affected due to one-side impact for the exterior building.

The seismic pounding provides displacement restrains on the impacting side, but may amplify displacement responses on the other side, particularly the response of 12-story building at the height levels above the impact level. Furthermore, the maximum responses in the short building are decreased in the impact and rebound directions. pounding has a considerable effect on the story shear response of the higher building in the stories upper than roof of the shorter structure. It is observed that pounding can make the story shear in the stories just higher than roof of the shorter building to surpass those of the lower ones. The reduction of seismic damage in beams, relative to no-pounding case, happens always in lower stories of both adjacent buildings along their common height. On the contrary, an increase of damage always is observed in the top stories of the shorter building and in the stories of the higher building on top of the roof of the shorter building. The time lag of the impact of the interior building with the right and left exterior buildings and different levels of impact reduce the impact interaction effect on the response demands of adjacent buildings in series, Synchronized impact at different levels of impact could maximize the adjacent building interaction and impact effects. Although pounding may sometimes reduce the overall structural response of short buildings and thus be considered beneficial, more often it will amplify the response significantly of the relative higher building irrespective the position of the building in the configuration alignment of adjacent building in series. The differences in height, period, the period ratio and relative alignment of adjacent buildings seem to be the crucial factors that affect the response of pounding buildings. Therefore, it is highly recommended to introduce into the codes conditions and provision for the assessment of the minimum required seismic separation and the pounding risk of buildings. Although some of the findings will be case study specific, many of the findings are highly relevant to many other adjacent buildings. Continued research is urgently needed in order to provide the engineering design profession with practical means to evaluate and mitigate the extremely hazardous effects of pounding.

Acknowledgements The authors would also like to record their indebtedness and thankfulness to the reviewers for their valuable and fruitful comments as well as for their powerful reading and suggestions. The financial support by Scientific Research Deanship, Taibah University Grant No. 7128/436 is gratefully acknowledged.

References

Abdel Raheem SE (2006) Seismic pounding between adjacent building structures. Electron J Struct Eng 6:66–74

Abdel Raheem SE (2009) Pounding mitigation and unseating prevention at expansion joint of isolated multi-span bridges. Eng Struct 31(10):2345–2356

Abdel Raheem SE (2013a) Evaluation and mitigation of earthquake induced pounding effects on adjacent buildings performance. In: 2013 World Congress on Advances in Structural Engineering and Mechanics—ASEM13 Congress, Jeju, Korea, Paper ID. MS509_201, 8–12 Sept

Abdel Raheem SE (2013b) Mitigation measures for seismic pounding effects on adjacent buildings responses. In: 4th conference of computational mechanics, structural dynamics and earthquake engineering—COMPDYN 2013, Kos Island, Greece, Paper ID. 1699, 12–14 June
Abdel Raheem SE (2014) Mitigation measures for earthquake induced pounding effects on seismic performance of adjacent buildings. Bull Earthq Eng 12:1705–1724
Abdel Raheem SE, Hayashikawa T (2013) Mitigation measures for expansion joint effects on seismic performance of bridge structures. In: The 13th East Asia-Pacific conference on structural engineering and construction (EASEC-13), Sapporo, Japan, Paper no. 286, 11–13 Sept
Abdel Raheem SE, Ahmed MMM, Ahmed MM, Abdel-shafy AGA (2018a) Evaluation of plan configuration irregularity effects on seismic response demands of L-shaped MRF buildings. Bull Earthq Eng 16(9):3845–3869. https://doi.org/10.1007/s10518-018-0319-7
Abdel Raheem SE, Fooly MYM, Abdel Shafy AGA, Abbas YA, Omar M, Abdel Latif MMS, Mahmoud S (2018b) Seismic pounding effects on adjacent buildings in series with different alignment configurations. Steel Compos Struct 28(3):289–308. https://doi.org/10.12989/scs.2018.28.3.289
Abrahamson N (2006) Program SeismoMatch v2–software capable of adjusting earthquake accelerograms to match a specific design response spectrum, using the wavelets algorithm proposed
American Society of Civil Engineers (ASCE) (2010) Minimum design loads for buildings and other structures. In: ASCE/SEI standard 7-10. American Society of Civil Engineers, Reston
American Society of Civil Engineers (ASCE) (2013) Seismic rehabilitation of existing buildings—ASCE/SEI 41-13. American Society of Civil Engineers (ASCE), Reston
Anagnostopoulos SA (1988) Pounding of buildings in series during earthquakes. Earthq Eng Struct Dyn 16:443–456
Anagnostopoulos SA, Karamaneas CE (2008) Use of collision shear walls to minimize seismic separation and to protect adjacent buildings from collapse due to earthquake-induced pounding. Earthq Eng Struct Dyn 37(12):1371–1388
Anagnostopoulos SA, Spiliopoulos KV (1992) An investigation of earthquake induced pounding between adjacent buildings. Earthq Eng Struct Dyn 21:289–302
Athanassiadou CJ, Penelis G, Kappos AJ (1994) Seismic response of adjacent buildings with similar or different dynamic characteristics. Earthq Spectra 10:293–317
Aykutozdemir (2018) http://www.aykutozdemir.com.tr/insaat/cekicleme-etkisi.html/cekicleme-etkisi-2-2. Accessed May 2018
Bertero VV (1987) Observations on structural pounding. In: Cassaro MA, Martinez Romero E (eds) The Mexico earthquakes-1985: factors involved and lessons learned. ASCE, New York, pp 264–278
Building Seismic Safety Council (BSSC) (2009) NEHRP recommended provisions for the development of seismic regulations for new buildings and other structures—FEMA P-750. Federal Emergency Management Agency, Washington
Bull D, Dhakal R, Cole G, Carr A (2010) Building pounding state of the art: Identifying structures vulnerable to pounding damage. New Zealand society for earthquake engineering annual conference, paperP11
Bureau of Indian Standards (IS) (2002) Indian standard criteria for earthquake resistant design of structures, part 1—general provisions and buildings, IS 1893, 5th edn. BIS, New Delhi
Cole G, Bull D, Dhakal R, Carr A (2010) Interbuilding pounding damage observed in the 2010 Darfield earthquake. Bull N Z Soc Earthq Eng 43(4):382–386
Cole G, Dhakal R, Carr A, Bull D (2011) Case studies of observed pounding damage during the 2010 Darfield earthquake. In: 9th Pacific conference on earthquake engineering building an earthquake-resilient society, Auckland, New Zealand, pp 14–16
Cole GL, Dhakal RP, Turner FM (2012) Building pounding damage observed in the 2011 Christchurch earthquake. Earthq Eng Struct Dyn 41(5):893–913. https://doi.org/10.1002/eqe.1164
Computers and Structures Inc. (CSI) (2013) CSI analysis reference manual for SAP2000, ETABS, and SAFE. Computers and Structures Inc., Walnut Creek
Computers and Structures Inc. (CSI) (2016) ETABS2016 v16.0.0: extended three dimensional analysis of building systems. Computers and Structures Inc., Berkeley
Davis R (1992) Pounding of buildings modelled by an impact oscillator. Earthq Eng Struct Dyn 21:253–274
DesRoches R, Muthukumar S (2002) Effect of pounding and restrainers on seismic response of multiple-frame bridges. J Struct Eng 128:860–869
Efraimiadou S, Hatzigeorgiou GD, Beskos DE (2013) Structural pounding between adjacent buildings subjected to strong ground motions. Part I: the effect of different structures arrangement. Earthq Eng Struct Dyn 42(10):1509–1528
Elwardany H, Seleemah A, Jankowski R (2017) Seismic pounding behavior of multi-story buildings in series considering the effect of infill panels. Eng Struct 144(1):139–150

European committee for Standardization (ECS) (2004) EC8: design of structures for earthquake resistance: general rules seismic actions and rules for buildings (EN 1998-1). ECS, Brussels

Favvata MJ (2017) Minimum required separation gap for adjacent RC frames with potential inter-story seismic pounding. Eng Struct 152:643–659

Federal Emergency Management Agency (FEMA) (2000) Prestandard and commentary for the seismic rehabilitation of buildings—FEMA 356. SAC Joint Venture, the Federal Emergency Management Agency, USA

Garcia DL (2004) Separation between adjacent nonlinear structures for prevention of seismic pounding. In: 13th world conference on earthquake engineering, Vancouver, CA, pp 1–6

Guo A, Li Z, Li H, Ou J (2009) Experimental and analytical study on pounding reduction of base-isolation highway bridges using MR dampers. Earthq Eng Struct Dyn 38(11):1307–1333

Guo A, Cui T, Li H (2012) Impact stiffness of the contact-element models for the pounding analysis of highway bridges: experimental evaluation. J Earthq Eng 16(8):1132–1160

Housing and Building National Research Center (ECP) (1993) ECP-201: Egyptian code for calculating loads and forces in structural work and masonry. Ministry of Housing, Utilities and Urban Planning, Cairo

Housing and Building National Research Center (ECP) (2007) ECP-203: Egyptian code for design and construction of reinforced concrete structures. Ministry of Housing, Utilities and Urban Planning, Cairo

Housing and Building National Research Center (ECP) (2008) ECP-201: Egyptian code for calculating loads and forces in structural work and masonry. Ministry of Housing, Utilities and Urban Planning, Cairo

Inel M, Ozmen H, Akyol E (2013) Observations on the building damages after 19 May 2011 Simav (Turkey) earthquake. Bull Earthq Eng 11:255–283

International Code Council (ICC) (2009) IBC: international building code. International Code Council (ICC), Birmingham

International Conference of Building Officials (ICBO) (1997) UBC97: uniform building code. In: Structural engineering design provisions, vol 2. Whittier, CA

Jankowski R (2006) Pounding force response spectrum under earthquake excitation. Eng Struct 28:1149–1161

Jankowski R (2009) Non-linear FEM analysis of earthquake-induced pounding between the main building and the stairway tower of the Olive View Hospital. Eng Struct 31(8):1851–1864

Jankowski R (2010) Experimental study on earthquake-induced pounding between structural elements made of different building materials. Earthq Eng Struct Dyn 39:343–354

Jeng V, Tzeng WL (2000) Assessment of seismic pounding hazard for Taipei City. Eng Struct 22(5):459–471

Jeng V, Kasai K, Maison BF (1992) A spectral difference method to estimate building separations to avoid pounding. Earthq Spectra 8:201–223

John A. Martin & Associates, Inc. (Johnmartin) (2018) Earthquake damage, Mexico City, September 19, 1985. http://www.johnmartin.com/earthquakes/eqshow/647003_08.htm. Accessed May 2018

Karayannis CG, Favvata MJ (2005) Earthquake-induced interaction between adjacent reinforced concrete structures with non-equal heights. Earthq Eng Struct Dyn 34(1):1–20. https://doi.org/10.1002/eqe.398

Kasai K, Maison BF (1991) Observation of structural pounding damage from 1989 Loma Prieta earthquake. In: 6th Canadian conference of earthquake engineering, pp 735–742

Kasai K, Maison BF (1997) Building pounding damage during the 1989 Loma Prieta earthquake. Eng Struct 19:195–207

Kawashima K, Shoji G (2000) Effect of restrainers to mitigate pounding between adjacent decks subjected to a strong ground motion. In: 12th world conference on earthquake engineering, New Zealand, Auckland, Paper no. 1435

Kawashima K, Unjoh S, Hoshikuma JI, Kosa K (2011) Damage of bridges due to the 2010 Maule, Chile, earthquake. J Earthq Eng 15:1036–1068

Khatiwada S, Chouw N (2013) A shake table investigation on interaction between buildings in a row. Coupled Syst Mech 2(2):175–190

Komodromos P, Polycarpou P, Papaloizou L, Phocas MC (2007) Response of Seismically Isolated Buildings Considering Poundings. Earthq Eng Struct Dyn 36(12):1605–1622

Kwon OS, Kim ES (2010) Evaluation of building period formulas for seismic design. Earthq Eng Struct Dyn 39(14):1569–1583

Mahmoud S, Jankowski R (2011) Linear viscoelastic modelling of damage-involved structural pounding during earthquakes. Key Eng Mater 452:357–360

Maison BF, Kasai K (1992) Dynamics of pounding when two buildings collide. Earthq Eng Struct Dyn 21:771–786

Mander JB, Priestley MJN, Park R (1988) Theoretical stress–strain model for confined concrete. J Struct Eng 114(8):1804–1826
Naserkhaki S, Ghorbania SD, Tolloeib DT (2013) Heavier adjacent building pounding due to earthquake excitation. Asian J Civ Eng (BHRC) 14(2):349–367
National Centers for Environmental Information (NCEI) (2018) ftp://ftp.ngdc.noaa.gov/hazards/cdroms/geohazards_v2/images/647003/jpg/64700308.jpg. Accessed May 2018
National Research Council of Canada (NRCC) (2005) NBCC: national building code of Canada, 12th edn. Canadian Commission on Building and Fire Codes, National Research Council of Canada, Ottawa
Openquake (2018) GEM—global earthquake model building taxonomy. https://taxonomy.openquake.org/terms/pounding-potential-pop. Accessed May 2018
Ozmen HB, Inel M, Cayci BT (2013) Engineering implications of the RC building damages after 2011 Van earthquakes. Earthq Struct 5(3):297–319. https://doi.org/10.12989/eas.2013.5.3.297.297
Shome N, Cornell CA, Bazzurro P, Carballo JE (1998) Earthquakes, records and nonlinear responses. Earthq Spectra 14(3):469–500
Pacific Earthquake Engineering Research Center (PEER) (2013). PEER NGA-West2 database. PEER report 2013/03, Pacific Earthquake Engineering Research Center, University of California, Berkeley
Papadrakakis M, Mouzakis H (1995) Earthquake simulator testing of pounding between adjacent buildings. Earthq Eng Struct Dyn 24:811–834
Polycarpou P, Komodromos P (2010) Earthquake-induced poundings of a seismically isolated building with adjacent structures. Eng Struct, Special Issue: Learning from structural failures 32(7):1937–1951
Rosenblueth E (1986) The 1985 earthquake: causes and effects in Mexico City. Concrete J 8:23–24
Shakya K, Wijeywickrema AC, Ohmachi T (2008) Mid-column seismic pounding of reinforced concrete buildings in a row considering effects of soil. In: 14th WCEE, Beijing, Paper ID 05-01-0056
Somerville PG (1998) Emerging art: earthquake ground motion. Geotech Earthq Eng Soil Dyn III ASCE Geotech Spec Publ 75(1):1–38
Watanabe G, Kawashima K (2004) Numerical simulation of pounding of bridge decks. In: The 13th world conference on earthquake engineering, Vancouver, BC, Canada

Affiliations

Shehata E. Abdel Raheem[1,2] · Mohammed Y. M. Fooly[2] · Aly G. A. Abdel Shafy[2] · Ahmed M. Taha[1] · Yousef A. Abbas[2] · Mohamed M. S. Abdel Latif[2]

[1] Civil Engineering Department, Engineering College, Taibah University, P.O. 344, Madinah 41411, Saudi Arabia

[2] Civil Engineering Department, Faculty of Engineering, Assiut University, Assiut 71516, Egypt